Journal of Controlled Release 324 (2020) 620–632

Contents lists available at ScienceDirect

Journal of Controlled Release

journal homepage: www.elsevier.com/locate/jconrel

Liposomal delivery of antibiotic loaded nucleic acid nanogels with enhanced drug loading and synergistic anti-inflammatory activity against *S. aureus* intracellular infections

Sybil Obuobi[a,*], Kjersti Julin[b], Elizabeth G.A. Fredheim[c], Mona Johannessen[b], Nataša Škalko-Basnet[a]

[a] Drug Transport and Delivery Research Group, Department of Pharmacy, UIT The Arctic University of Norway, Tromsø, Norway
[b] Host Microbe Interaction research group, Department of Medical Biology, UIT The Arctic University of Norway, Tromsø, Norway
[c] Microbial Pharmacology and Population Biology, Department of Pharmacy, UIT The Arctic University of Norway, Tromsø, Norway

ARTICLE INFO

Keywords:
Nucleic acid nanogels
DNA
Staphylococcus aureus
Controlled release
Persistent infections
Liposomes

ABSTRACT

The persistence of *Staphylococcus aureus* has been accredited to its ability to escape immune response *via* host cell invasion. Despite the efficacy of many antibiotics against *S. aureus*, the high extracellular concentrations of conventional antibiotics required for bactericidal activity is limited by their low cellular accumulation and poor intracellular retention. While nanocarriers have received tremendous attention for antibiotic delivery against persistent pathogens, they suffer daunting challenges such as low drug loading, poor retention and untimely release of hydrophilic cargos. Here, a hybrid system (Van_DNL) is fabricated wherein nucleic acid nanogels are caged within a liposomal vesicle for antibiotic delivery. The central principle of this approach relies on exploiting non-covalent electrostatic interactions between cationic cargos and polyanionic DNA to immobilize antibiotics and enable precise temporal release against intracellular *S. aureus*. *In vitro* characterization of Van_DNL revealed a stable homogenous formulation with circular morphology and enhanced vancomycin loading efficiency. The hybrid system significantly sustained the release of vancomycin over 24 h compared to liposomal or nanogel controls. Under enzymatic conditions relevant to *S. aureus* infections, lipase triggered release of vancomycin was observed from the hybrid. While using Van_DNL to treat *S. aureus* infected macrophages, a dose dependent reduction in intracellular bacterial load was observed over 24 h and exposure to Van_DNL for 48 h caused negligible cellular toxicity. Pre-treatment of macrophages with the antimicrobial hybrid resulted in a strong anti-inflammatory activity in synergy with vancomycin following endotoxin stimulation. Conceptually, these findings highlight these hybrids as a unique and universal platform for synergistic antimicrobial and anti-inflammatory therapy against persistent infections.

1. Introduction

The rising incidence of persistent infections and multidrug-resistant bacteria constitute a major threat to global health and has raised concerns over the prospects of a post-antibiotic era [1]. A large fraction of community and nosocomial infections are attributable to *S. aureus* and its methicillin-resistant strain (MRSA), with significant percentages of the global population notoriously being persistent (20%) or intermittent carriers (60%) [2]. Treatment of *S. aureus* is especially challenging as the pathogen is able to escape immune response *via* host cell invasion where it has life-long protection from antimicrobial therapy [3]. Because many conventional antimicrobials have restricted intracellular penetration or low retention, more than two-thirds of prescribed antibiotics are ineffective and cause severe systemic toxicity [4,5]. Treatment with sub-optimal dosing, not reaching bactericidal intracellular concentrations enhances the risk for developing drug resistant infections. There is therefore an urgent need to develop drug delivery platforms that can enhance the efficacy of conventional antibiotics against intracellular infections.

Nanomaterial-enabled drug delivery systems have been extensively explored to improve uptake, enhance targeting and bioavailability of several drug molecules [6]. Among the many nanocarriers of interest, core-shell drug carriers such as liposomes are among the most successful commercialized antimicrobial therapeutics [7,8]. Despite their success, low drug loading content, poor retention and untimely release of hydrophilic cargos remain major roadblocks of liposomal products

* Corresponding author.
E-mail address: sybil.obuobi@uit.no (S. Obuobi).

https://doi.org/10.1016/j.jconrel.2020.06.002
Received 11 March 2020; Received in revised form 10 May 2020
Available online 07 June 2020

[9]. To improve drug loading, a popular approach *via* remote active loading of drugs into preformed liposomes uses pH gradients and potential differences across liposomal membranes [10]. However, this is reserved for drugs with protonizable amines and is ineffective where pH and ion gradients do not apply. Recent approaches to facilitate drug accumulation *via* secure cargo loading within liposomes include smart strategies to covalently functionalize cargos to cue responsive linkers for site-specific drug release [11,12]. Nevertheless, such strategies require specific tedious covalent conjugations, toxic crosslinkers and harsh purification steps. On the other hand, advancing trends within nanomedicine using deoxyribonucleic acid based nanocarriers for intracellular drug delivery has received much attention for its simplicity and specificity [13,14]. Recent literature on the development of DNA nanostructures (*e.g.* tetrahedrons and nanogels) demonstrate defined control over hydrodynamic size/shape, with high payload capacity reaching maximal efficacy, low toxicity, efficient intracellular delivery and immune-modulatory applications [15–17]. These nanomaterials are amenable to loading DNA-binding drugs *via* intercalation and electrostatic interactions with high efficiency and drug efficacy [18–21]. For instance, the high binding affinity between crosslinked DNA nanostructures and antimicrobial peptides was recently exploited for the topical treatment of *S. aureus* [22]. However, relying on reversible non-covalent electrostatic bonds for intracellular drug delivery is highly prone to premature extracellular release which can compromise performance [23]. Additionally, crossing the limits for drug loading of cationic ligands (drug: DNA) is associated with complex formation, precipitation and poorer intracellular penetration.

The development of antimicrobial drug delivery systems controlled by the microenvironment of bacteria pathogens can be exploited to induce or initiate antibiotic release [24]. Such virulence factors (*e.g.* lipases and DNase) are produced in abundance by bacteria to impair cell function and elicit host damage [25]. The exploitation of these toxins has been widely reported as stimuli to trigger the release of entrapped cargos from liposomes and DNA-based nanomaterials. For instance, Yang and co-workers recently demonstrated an enhanced release of vancomycin from liposome coated mesoporous nanoparticles in the presence of bacteria lipases [26]. Several other nanocarriers have been shown to respond to bacterial lipases [27–29]. Pan and co-workers studied the nuclease digestion of gemcitabine-containing DNA nanogels over 24 h [30]. After incubating the nanocarriers in DNASE II, the authors report an almost complete degradation of the nanogels using PAGE analysis. Simultaneous detection and killing of *S. aureus* pathogens was also shown using DNA nanoscaffolds loaded with actinomycin D [13]. The authors demonstrated degradation of the nanostructure in response to DNase enzymes which was responsible for the release and effective killing of the infectious bacteria. Hybrids developed by combining these strategies can enable the fabrication of advanced antimicrobial platforms with enhanced potency against bacterial infections.

Recently, Chen and colleagues developed a hydrogel enveloped liposomal nanostructures with high drug loading and enhanced delivery of nucleic acids and proteins [31]. Inspired by this approach, we envisioned that non-covalent drug loading and subsequent entrapment of nucleic acid nanogels within liposomal vesicles could facilitate high encapsulation efficiency and enable “on-demand” release of cationic drugs. In this study, we designed and fabricated nanostructured hybrid system wherein nucleic acid nanogels are caged within a liposomal vesicle for the intracellular delivery of vancomycin. We demonstrated that by exploiting the non-covalent interactions between entrapped DNA nanostructures and vancomycin, the hybrids achieved higher antibiotic loading efficiencies than the liposomal controls. Acting as a barrier to rapid drug loss, the hybrids sustained the release of vancomycin under physiological conditions and, upon exposure to enzymatic proteins, rapidly degrade to provide control over release kinetics in microbial environments. Effective inhibition of planktonic and intracellular *S. aureus* in a dose dependent manner was observed over 24 h in *in vitro* models of infection and the hybrids caused negligible cellular toxicity over 48 h. Pre-treatment of macrophages with the antimicrobial hybrid resulted in a potent anti-inflammatory activity in synergy with vancomycin following endotoxin stimulation. Notably, the potent anti-oxidant activity of the blank hybrids did not perturb the oxidative stress mediated antibacterial mechanism of the antimicrobial cargo. These findings underscore the versatility of the hybrid system as an innovative platform for antibiotic loading and therapy against persistent infections which can be adapted for other pathological conditions and further developed as multifunctional co-delivery systems.

2. Experimental section

2.1. Fabrication and characterization of the hybrids

Blank and vancomycin-loaded DNA nanogels were prepared by adopting a two-step annealing method, as previously published [15]. Briefly, the nanostructures were formed by mixing stochiometric concentrations of each single strand oligonucleotide (Integrated DNA Technologies, Belgium) in 1× encapsulation buffer [32] (EB) (5 mM Tris-HCL, 1 mM EDTA, 10 mM $MgCl_2$, 10 mM NaCl) (Sigma Aldrich, Norway) to achieve final concentrations of 1 μM (Y-SAB), 4 μM (Y-SAF) and 6.5 μM (L-SAC) of the monomers, respectively. The samples were hybridized at 95 °C and slowly cooled to 4 °C for 2.5 h. Thereafter, equal volumes of the monomers were added to an equal volume of buffer or vancomycin (Sigma Aldrich, Norway) to form the blank nanogel (DNG) or vancomycin loaded nanogel (Van_DNG) formulations. The samples were heated at 95 °C and quickly cooled to 4 °C for 3.5 h. The self-assembly of the nanostructures and formation of the nanogel was confirmed using agarose electrophoresis (100 V for 45 min) and imaged using the GelDoc XR+ (BIORAD, Norway).

Liposomes were prepared using standard techniques. Briefly, lipid films were prepared using the thin-film hydration method by dissolving pure soy phosphatidylcholine (Lipoid S100) (Lipoid GmbH, Ludwigshafen, Germany) in methanol (Sigma Aldrich, Norway) and placing the solution under vacuum at 45 °C [33]. After 1.5 h, the film was rehydrated with blank buffer, DNG or Van_DNG to achieve a theoretical lipid concentration of 10 mg/mL. The solutions were extruded 5× through 800 nm, 400 nm and 200 nm polycarbonate membranes (Sigma Aldrich, Norway) and stored at 4 °C [33]. The liposomes were purified by dialysis against 1× EB buffer to remove the un-encapsulated drug and DNA using membranes with a cut-off of 12–14 kDa (Thermo Fischer Scientific, Norway) and 1000 kDa (Thermo Fischer Scientific, Norway) respectively. The samples were stored at 4 °C until further used. The size distribution and zeta potential were determined *via* dynamic light scattering (DLS) using the NanoZS Zetasizer (Malvern) with standard settings [34]. The stability of the liposomes was performed by monitoring changes in size,zeta potential and PDI.

For TEM measurements, the formulations were deposited on glow discharged 200 or 400 mesh carbon-coated grids for 5 min and stained with uranyless (Electron Microscopy Sciences, USA) for 10–40 s. The samples were allowed to air-dry for 30 min and imaged using the HT7800 (Hitachi, Japan) at 20–120 kV acceleration voltage equipped with Morada digital camera.

2.2. Encapsulation efficiency and lipid content determination

The encapsulation efficiency (EE%) of vancomycin or DNA was calculated using the equation:

$$EE\% = (C_{encap}/C_{total}) \times 100\%$$

where C_{encap} refers to the measured concentration of vancomycin or DNA obtained after dialysis and C_{total} is the concentration of vancomycin or DNA in an equal volume of the formulations before dialysis.

Liposomal solutions were disrupted using methanol (90%$^{v}/_{v}$) and the samples containing DNA were purified *via* centrifugation using centrifugal filters (50 kDa) (Sigma Aldrich, Norway). The concentration

of vancomycin was determined *via* UV absorbance (280 nm) (Agilent 8453, USA) with a pre-determined calibration curve using the flow-through obtained.

To determine the EE% of DNA, the picogreen (Thermo Fischer Scientific, Norway) assay method was used. After disruption with methanol, 50 μL of picogreeen was added to an equal volume of the sample and incubated for 5 min in the dark. The concentration of DNA was then quantified using fluorescence (Ex. 480 nm, Em. 520 nm) measurements. The lipid concentration of each formulation was also determined *via* fluorescence using the phospholipid quantification kit (Sigma Aldrich, Norway) by following the manufacturer's protocol (Ex. 535 nm, Em. 587 nm). All fluorescence measurements were performed on Spark multimode microplate reader (Männendorf, Switzerland).

2.3. Binding affinity determination

The interactions between vancomycin and the DNA nanostructures was studied in 1× EB by recording changes in UV absorbance. Briefly, 100 μg/mL of vancomycin and 1 μM of Y-SAF monomer was prepared. The monomer was diluted two-folds and added to an equal volume of vancomycin to achieve final concentrations of 0.5 μM to 0.0625 μM DNA and 50 μM vancomycin. The spectra analysed using the plate reader at 280 nm for vancomycin alone served as the control.

For Förster resonance energy transfer (FRET) assay, BODIPY labelled vancomycin (BODIPY-Van) (Fischer Scientific, Norway) was incubated with Alexa-594 labelled DNA (IDT, Belgium) nanogel or Alexa-594 labelled Y-SAF monomer at RT and excited at 435 nm. A reduction in the donor emission at 514 nm with a corresponding increase in the acceptor emission at 620 nm was indicative of FRET.

DLS was performed to monitor the changes in the hydrodynamic size of Y-SAF monomer in the presence of increasing concentrations of vancomycin in 1× EB.

2.4. In vitro drug release determination

The release profile of vancomycin from the formulations was obtained using a vertical static Franz Diffusion Cell apparatus (PermeGear, USA) equipped with a 5 mL acceptor chamber. The donor chamber was loaded with 700 μL of Van_DNL with or without 1 mg/mL Lipase (from wheat germ, ~0.1 U/mL) (Sigma Aldrich, Norway) and mounted on a cellophane membrane barrier (Zellglas, Germany). As a control, the release of vancomycin from the nanogels (Van_DNG) or liposomal formulation alone (Van_L) was also studied. The receptor chamber was filled with phosphate buffered saline (pH 7.4) and maintained at 32 °C under constant stirring. Lipase sensitive release profiles of the liposomes was studied by adding 5%$^{v}/_{v}$ of 20 mg/mL Lipase solution to achieve a final concentration of 1 mg/mL in the donor chamber. Samples (500 μL) were withdrawn at predetermined time points from the receptor chamber and then replaced with an equivalent volume of fresh buffer. The concentration of vancomycin released into the receptor chamber was determined *via* absorbance and reported as the mean ± SD using triplicate readings (n = 3). At the end of 24 h, the concentration of vancomycin remaining in the donor chamber was quantified after disrupting the liposomes and removing DNA [34].

2.5. Overnight culture growth assay

Bacterial viability was determined after exposure to the formulations using standard broth dilution tests. Briefly, *S. aureus* (MSSA476) (ATCC, USA) was grown in Mueller Hinton Broth (MHB) medium (Sigma Aldrich, Norway) to the mid log phase and diluted in fresh MHB to achieve a final bacterial CFU of 3 × 10^5 CFU/mL [35]. To each well of a 96 well plate, 50 μL of OD-adjusted *S. aureus* was added to an equal volume of formulations to achieve final vancomycin concentrations ranging from 0.06 μg/mL to 4 μg/mL. The plates were incubated at 37 °C under continuous shaking (100 rpm) for 16 h and the bacterial viability determined by measuring the optical density at 600 nm on a Spark multimode microplate reader (Männendorf, Switzerland) to determine the minimum inhibitory concentration (MIC). The percentage reduction in bacterial cell viability was calculated of the growth control group where bacterial cells were treated without the formulations. All experiments were performed in triplicate.

2.6. Time kill assay determination

Time-kill curves were obtained by culturing *S. aureus* in the presence of the hybrid formulation, Van_DNL alone at 1 x MIC to 4 x MIC. Bacterial cultures were prepared in MHB from bacteria grown to the mid-log phase and then diluted to obtain a final inoculum concentration of 3 × 10^6 CFU/mL. For each concentration, 500 μL of bacterial culture was added to 500 μL of the formulations and incubated under continuous shaking of 100 rpm at 37 °C. At predetermined time points, 10 μL samples were taken at 0 h, 1 h, 2 h, 4 h, 8 h and 24 h, serially dilute 10-fold to determine the number of viable bacteria. For controls, bacteria growth was determined in the presence of MHB buffer alone. The viable bacterial colonies were determined by plating 20 μL drops of each dilution on MHB agar plates (Sigma Aldrich, Norway) in triplicates. The plates were further incubated for 24 h. To quantify the number of viable bacteria the following equation was used: Viable count (CFU/mL) = dilution factor x [average number of colonies per drop/ volume of drop (0.02 mL)]. The experiments were performed in triplicates.

2.7. In vitro uptake and subcellular distribution

The intracellular trafficking profile of the Van_DNL in RAW 264.7 cells (Sigma Aldrich, Norway) was examined using confocal microscopy. Raw 264.7 cells (passage 6–10) were seeded at a density of 1 × 10^5 cells per well in 8 well chambers (Thermo-Fischer, Norway) and incubated for 24 h (37 °C, 5% CO_2). After washing each well twice with phosphate buffered saline (PBS) (Sigma Aldrich, Norway), the cells were treated with the Van_DNL for 12 h. After 12 h, the cells were washed with PBS, stained with Hoeschst 333342 (Thermo Fischer Scientific, Norway) and incubated for 15 min. After 15 mins, the cells were washed and incubated with LysoTracker Red dye (Thermo Fischer Scientific, Norway) and imaged using the Zeiss LSM 800 confocal microscope (Germany).

2.8. Intracellular antimicrobial activity

To test the intracellular antimicrobial activity of the Van_DNL formulation, RAW 264.7 cells (passage 6–10) were seeded into 12-well plates at a density of 2.5 × 10^5 cells per well in DMEM HG (supplemented with 10% *v*/v Fetal Bovine Serum and 1% Pen/Strep) (Sigma Aldrich, Norway) and incubated for 24 h (37 °C, 5% CO_2). *S. aureus* was grown to the mid-log phase in tryptic soy broth (TSB) (Sigma Aldrich, Norway) broth. The cells were collected *via* centrifugation and then diluted in PBS. After adjusting the bacteria concentration to 3 × 10^7 CFU/mL, *S. aureus* was diluted in DMEM (without Pen/Strep) and added to each well at a MOI of 10. After infecting the cells for 30 mins, the cells were washed and incubated with DMEM (supplemented with 2% *v*/v Fetal Bovine Serum) and gentamycin (100 μg/mL) for 1 h to eliminate extracellular bacteria. The cells were washed and treated with Van_DNL at doses of 1, 10 and 100 μg/mL for 18 h. After 18 h, the cells were washed again and lysed using PBS containing triton X (0.2%$^{v}/_{v}$) (Sigma Aldrich, Norway) for 30 mins to determine the intracellular activity of the formulation. The lysed cells were diluted in PBS and the number of viable bacteria enumerated by plating the lysates on MHB agar plates. After 24 h, the number of viable counts were determined by visually counting the cells and the loss in bacteria colonies calculated as a percentage of the untreated control.

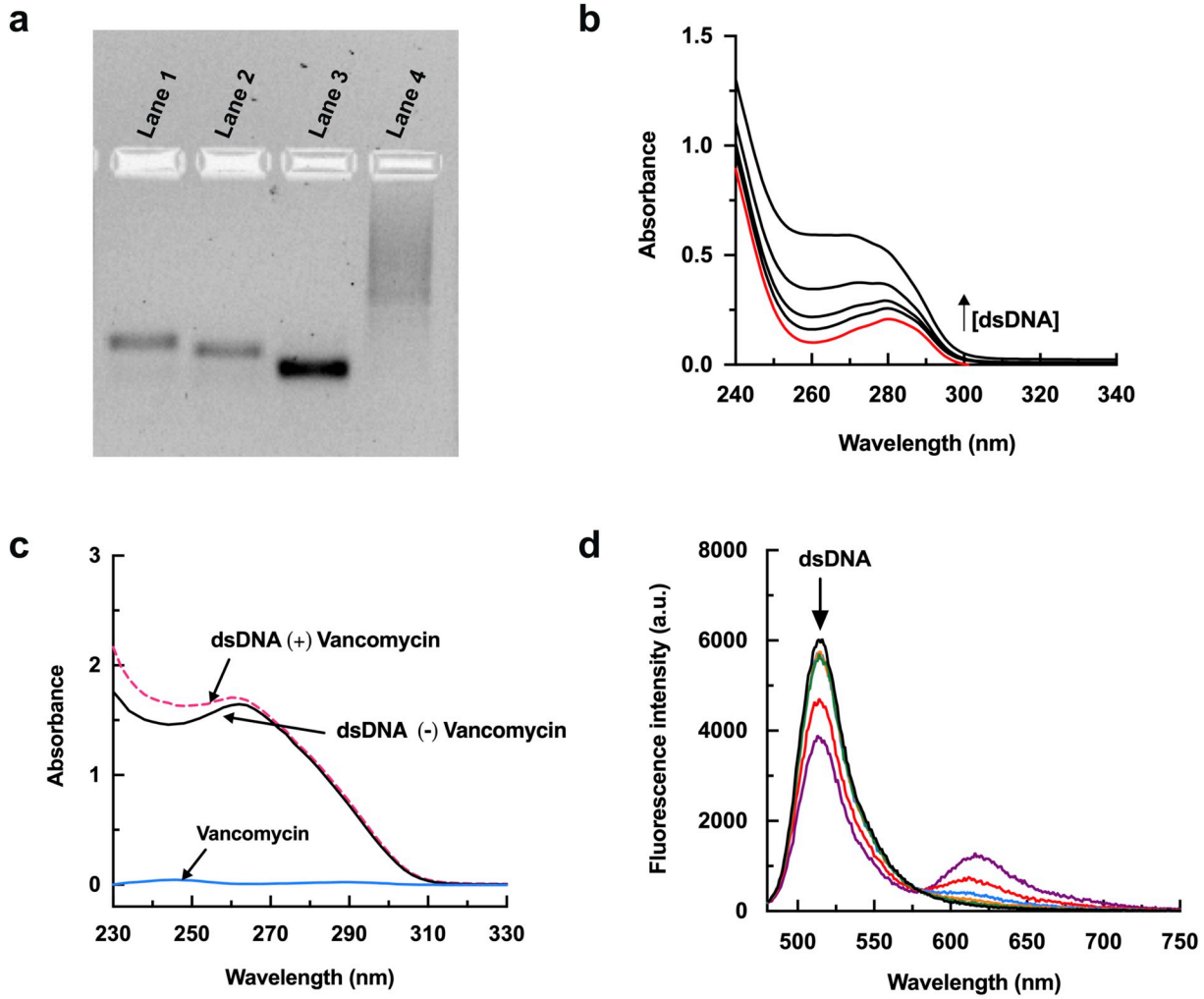

Fig. 1. Fabrication of DNA nanogels and binding studies. a) Gel electrophoresis of hybridized Y-SAF (Lane 1), Y-SAB (Lane 2), L-SAC (Lane 3) and DNA nanogel (Lane 4). b) Effect of increasing dsDNA (Y-SAF) on UV spectra of vancomycin (280 nm). c) Effect of vancomycin on UV spectra of dsDNA (L-SAC). d) FRET analysis with Alexa-594 Y-SAF (acceptor) and BODIPY vancomycin (donor).

2.9. In vitro cytotoxicity assay

The cytoxicity of Van_DNL was evaluated in murine RAW 264.7 cells (passage 6–10) over 48 h. Briefly, the cells were seeded at 6000 cells/well in 96-well plates and incubated for 24 h (37 °C, 5% CO_2). Thereafter, the cells were washed with PBS and incubated with increasing concentrations of Van_DNL with and without vancomycin. After 48 h incubation, the percentage cell viability was quantified using MTT assay (Sigma Aldrich, Norway) by following standard protocols. After incubating the cells with MTT solution (10 mg/mL) diluted in DMEM (1:10) for 2 h, the cells were washed and the purple formazan crystals dissolved with DMSO (100 μL) (Sigma Aldrich, Norway). Absorbance readings were recorded at 570 nm and the number of viable cells expressed as a percentage of the control.

2.10. Anti-inflammatory activity

To evaluate the anti-inflammatory activity of Van_DNL, RAW 264.7 cells (passage 6–10) were seeded in 24 well plates at 40,000 cells per well and allowed to attach for 24 h (37 °C, 5% CO_2) in DMEM HG (supplemented with 10% *v*/v Fetal Bovine Serum and 1% Pen/Strep). Afterwards the cells were pre-treated with the formulations in DMEM HG (supplemented with 3% v/v Fetal Bovine Serum) for 24 h. Thereafter, the cells were washed with PBS and stimulated with lipopolysaccharide (LPS; *Escherichia coli* O55:B5, Sigma Aldrich, Norway) at 500 ng/mL. After 12 h the media was collected for cytokine analysis. In another set of experiments, the cells were allowed to attach for 24 h. Thereafter, the cells were starved by incubating in DMEM HG (supplemented with 3% *v*/v Fetal Bovine Serum) for another 24 h. The cells were then washed with PBS and then co-treated with LPS and the formulations for 12 h. The media was collected, centrifuged and the supernatant collected for analysis.

After pre−/co- treatment with the formulation, the amount of IL-6 released was quantified to determine the anti-inflammatory activity of the formulations using ELISA Kits (Thermo Fischer Scientific, Norway) according to the manufacturer's guidelines.

2.11. Detection of ROS level

The Dichloro-dihydro-fluorescein diacetate (DCFH-DA) (Sigma Aldrich, Norway) assay was used to determine reactive oxygen species (ROS) production from the macrophage cells. Briefly, RAW264.7 cells were pre-treated with Van_DNL as previously described for the IL-6 ELISA test. After treatment, the cells were stimulated with LPS for 12 h. Thereafter the media was removed, the cells were washed and then incubated with DCFH-DA for 25 min. The fluorescence intensity was measured using the Spark multimode microplate reader (Männendorf, Switzerland) to evaluate the ROX produced by the cells.

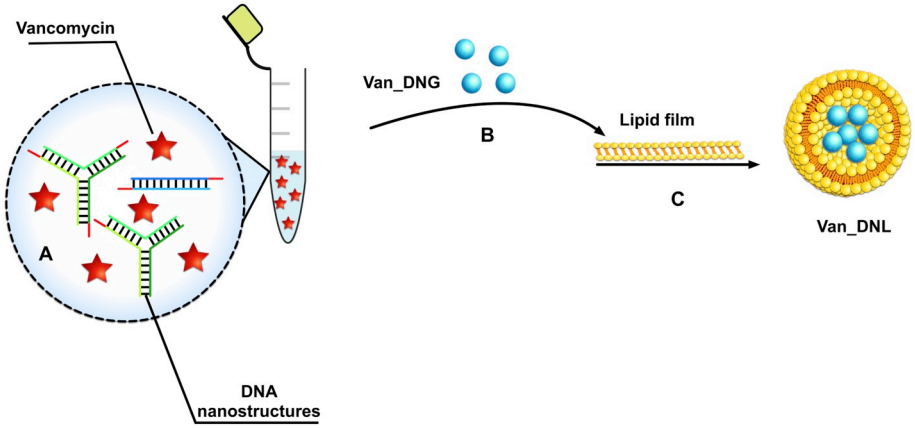

Fig. 2. Development of antimicrobial hybrids. (A) Fabrication of antibiotic loaded nanogels through non-covalent electrostatic interactions in parallel with Watson Crick base-pairing and (B) subsequent rehydration of lipid films (C) to produce the antimicrobial hybrids.

2.12. Statistics

Data was represented as the mean standard deviations and analysed using GraphPad Prism 8 (La Jolla, CA). The statistical significance among the groups was determined using the two-sample student *t*-test and one-way ANOVA analysis. Multiple comparisons were done using Dunnett's test. The results were reported as statistically significant for $p < .05$.

3. Results and discussion

3.1. Synthesis of the nanogels and characterization of their binding to vancomycin

The formation of the DNA nanostructures and their self-assembled nanogel products used in the preparation of Van_DNL was achieved *via* self-assembly of complementary ssDNA sequences (Table S1). The products were analysed using agarose gel electrophoresis as shown in Fig. 1a. A single band was shown for the individual monomers (Lane 1–3) indicating the absence of side products and complete hybridization of the strands (Fig. 1a). A smear band of higher molecular weight products were observed (Lane 4) due to the slower migration of the nanogel product than the individual monomers, an indication of the self-assembly of the nanostructures to successfully form polydisperse nanogels. This observation is similar to previous reports on oligonucleotide rapid self-assembly of DNA nanostructures for nanogel fabrication [36–38]. Moreover, the self-assembly of the nanogels offers a simple and non-toxic strategy over other nanocarriers which rely on chemical functionalization or are challenged by toxic initiators or long synthesis time [29,39].

Next, the interactions between vancomycin and the DNA nanogels was probed by measuring changes in the UV spectra of vancomycin and dsDNA. As shown in Fig. 1b, gradual addition of the DNA nanostructures resulted in a corresponding increase in absorbance bands (hyperchromic effect) of vancomycin. A similar hyperchromic effect was observed when vancomycin was added to the dsDNA (Fig. 1c). In both instances a characteristic red-shift of 1–11 nm (vancomycin) and 2 nm (DNA spectra) was recorded indicating the presence of non-covalent interactions (*e.g.* aromatic stacking) between vancomycin and the dsDNA nanostructures. FRET (Fig. 1d) characterization of the molecular interactions between vancomycin and the nanostructures was also investigated using BODIPY labelled vancomycin as the donor and Alexa_594 labelled DNA as the acceptor. Changes in the fluorescence intensity of BODIPY labelled vancomycin (2 μM) alone and in the presence of increasing concentrations of Alexa_594 labelled DNA nanostructures was monitored by exciting the donor at 435 nm. A progressive increase in the acceptor fluorescence intensity at 620 nm (dsDNA) and corresponding quenching of the donor fluorescence at 514 nm (vancomycin) was observed. There was approximately 87.60 ± 5.07% increase in fluorescence for the acceptor at the highest concentrations of the nanostructures as a result of the resonance energy transfer between the donor and acceptor. All together, these results demonstrate the close proximity of the chromophores of vancomycin to the bases of the DNA nanostructures attributable to aromatic stacking/ hydrogen bonding/ electrostatic/hydrophobic interactions and agrees with reports on the main chemical driving forces for vancomycin-DNA interactions [40,41]. For instance Kong and co-workers demonstrated that vancomycin possessed the ability to promote the aggregation of DNA using Rayleigh scattering and resonance nonlinear scattering (a highly sensitive method) [40]. As the last-resort antibiotic for the treatment of severe infections caused by gram-positive bacteria, our observations further confirm that vancomycin can be efficiently incorporated into the hybrid system. Other considerations made include that in comparison with previously trialed antimicrobial peptide L12 (MIC: 8 μM), the higher potency of vancomycin (MIC < 1 μM) against *S. aureus* is attractive when complexed with DNA thus, vancomycin was used as the model drug [22].

3.2. Synthesis and characterization of Van_DNL

As shown in Fig. 2, Van_DNL were synthesized by following a three-step self-assembly procedure. Firstly (step A), the monomeric nanostructures Y-SAF (main scaffold), L-SAC (linker) and Y-SAB (terminating unit) were synthesized individually, mixed together with vancomycin (Van_DNG) or buffer solutions (DNG) and then hybridized to promote *in situ* drug entrapment and nanogel formation (step B). Pre-formed lipid films (step C) prepared using the thin-film method were then hydrated with the DNA nanogels to obtain the antimicrobial hybrids (Van_DNL) or blank hybrids (DNL).

To design a hybrid tailored against intracellular bacterial infections, adequate control of size and surface charge is critical for uptake. We selected the three nanostructures due to the relatively small size of the nanogel construct reported to facilitated intracellular uptake [15]. To prevent the formation of complexes of larger sizes at high concentrations of vancomycin, we investigated the effect of antibiotic loading on the size of the nanogels using DLS. As shown in Fig. 3a, we observed no significant increase in the size of the nanogels below 2460 μg/mL of vancomycin. Conversely, a significant increase in average size of the nanogel from 76.73 ± 16.76 nm to 482.30 ± 40.53 nm (2460 μg/mL) and 579.93 ± 57.46 nm (at 4920 μg/mL), respectively, was observed clearly demonstrating the binding affinity between the DNA nanogels and vancomycin.

Since we aimed to prepare hybrids of ~200 nm size, we then sought to address the impact of drug concentration on the entrapment of the

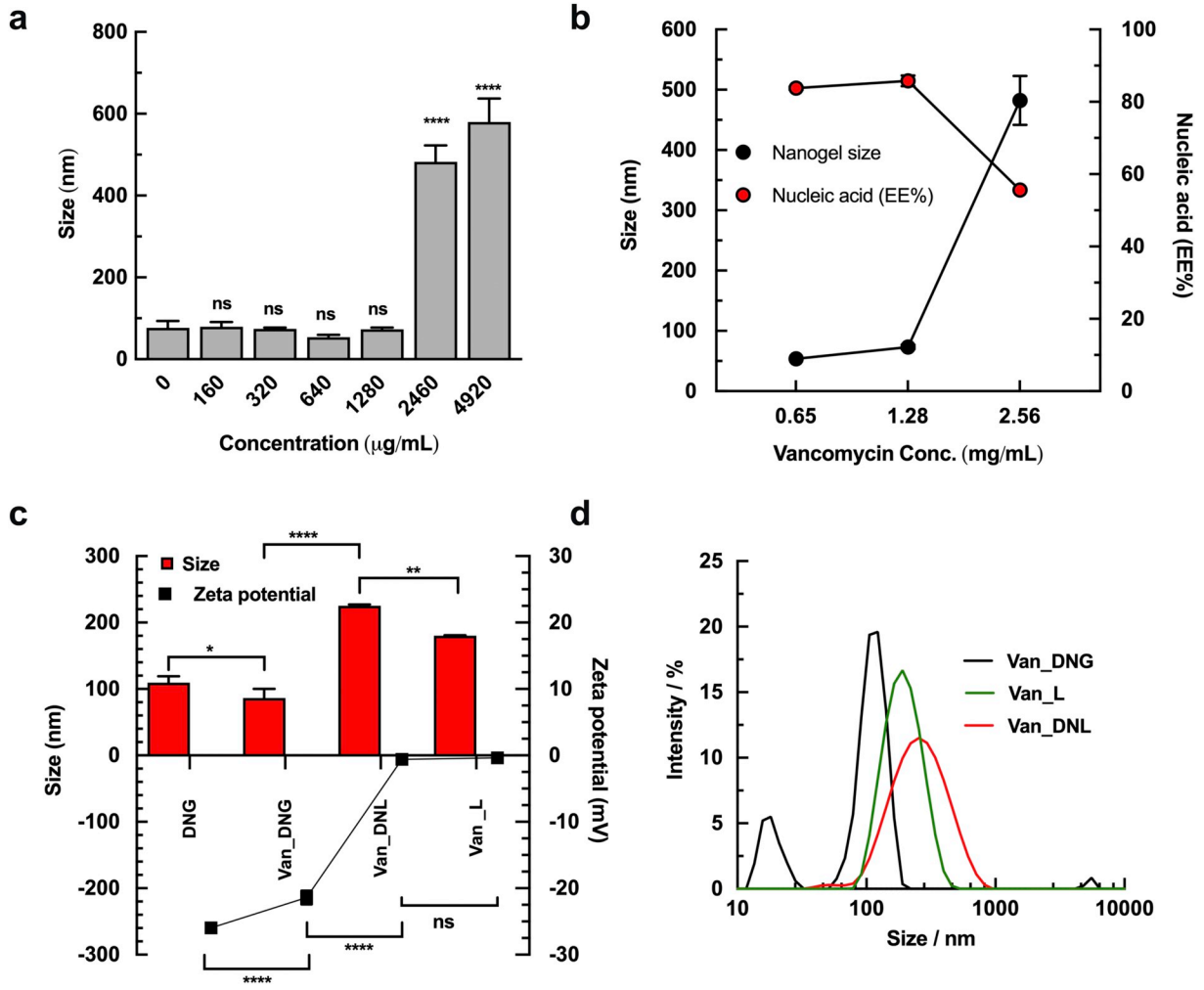

Fig. 3. Fabrication of hybrids and characterization of the antibiotic nanogels and hybrids. a) Effect of vancomycin on hydrodynamic diameter of the nanogels. b) Effect of nanogel size on nucleic acid entrapment efficiency. c) Hydrodynamic diameter and zeta potential measurements of the formulations. d) Size distribution of the vancomycin loaded hybrids, liposome and DNA nanogel formulations.

DNA nanogel within the hybrid after extrusion by quantifying dsDNA. Formulations prepared with three different concentrations of vancomycin were selected for analysis. Soy phosphatidyl choline (SPC, > 94% purity), a neutral lipid, was chosen in the fabrication of Van_DNL to prevent structural distortion of the nanogel which we hypothesized could influence antibiotic entrapment. As shown in Fig. 3b, nucleic acid entrapment efficiency was 83.78 ± 0.511% and 85.78 ± 1.47% for Van_DNL at vancomycin doses of 640 μg/mL and 1280 μg/mL, respectively. A significant reduction in nucleic acid entrapment to 55.61 ± 0.158% was observed above 1280 μg/mL stemming from the formation of larger nanocomplexes which supports the DLS results. Thus, we selected vancomycin dose of 1280 μg/mL for synthesizing Van_DNL.

Next, to further characterize the nanogel, liposomal and hybrid formulations, DLS was performed to determine the differences in size and zeta potential. As shown in Fig. 3c, vancomycin loading into nanogel resulted in a significant size reduction (from 109.33 ± 9.66 nm to 86.23 ± 14.02 nm) and zeta potential (from −25.98 ± 0.39 to −21.40 ± 1.01) for Van_DNG. This observation is attributable to the neutralization of the anionic surface potential and condensation of the nanogel. The subsequent entrapment of nanogel within the liposomes to form the Van_DNL resulted in a significant increase in the hydrodynamic diameter in comparison to Van_L or Van_DNG formulations. For instance, a significant change from 180.27 ± 0.67 nm (Van_L) to 225.20 ± 1.91 nm (Van_DNL) was recorded which clearly demonstrates the entrapment of the DNA nanogel. Moreover, liposomal vesicle shielded the highly negative surface charge of the nucleic acids and resulted in a significant change in zeta potential from −21.40 ± 1.01 to −0.60 ± 0.30 as shown in Fig. 3c. Additionally, Van_DNL showed a narrow and homogenous (PDI: 0.20 ± 0.01) size distribution compared to the Van_DNG formulation exhibiting a polydispersity index of 0.50 ± 0.04 (Fig. 3d). Recent fabrication of DNA coated mesoporous nanoparticles demonstrated a significant increase in size from 191 ± 8 to 216 ± 25 nm due to the coated DNA layer [42]. The authors also reported a change in the surface potential for the amino functionalize nanoparticles which became more negative following DNA functionalization. Their observations were similar to this present work wherein the lipid bilayer coating resulted in an increased size while maintaining a low PDI and good homogeneity. The neutralized surface potential also provides a clear indication of the successful nanogel coating.

Encapsulation efficiency (EE%) measurements were conducted to compare the entrapment efficiency of vancomycin in the formulations. As shown in Fig. 4a, Van_DNL displayed an EE % of 76.59 ± 3.44% which was significantly higher than the Van_L control group (64.64 ± 0.73%).

Comparatively, we observed no significant difference between the lipid concentration in the two formulations. The observed increment in EE % can be attributable to increased drug concentration in the liposomal core due to the non-covalent binding of vancomycin to the

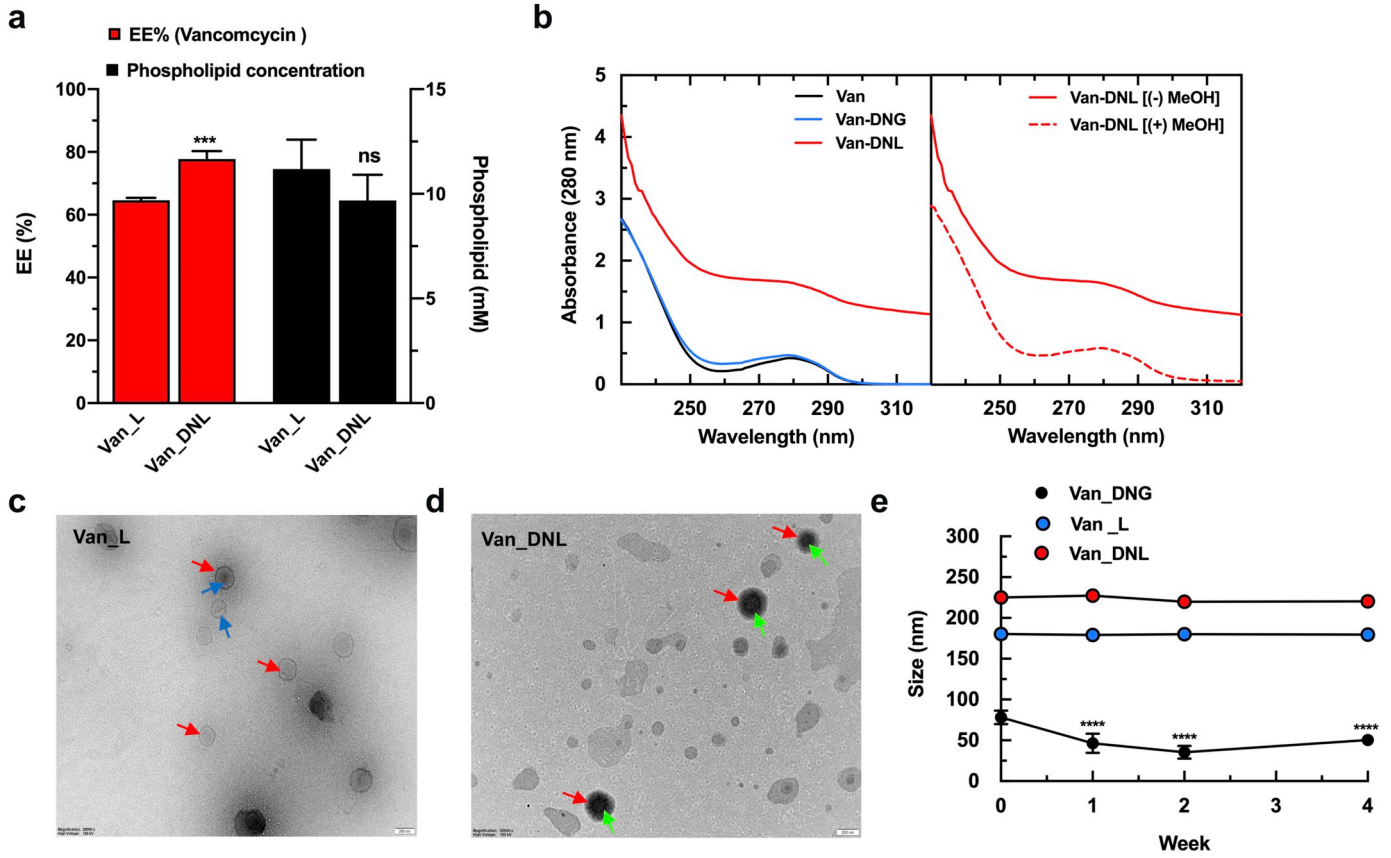

Fig. 4. Drug entrapment and stability of the hybrids. a) Entrapment efficiency of vancomycin in the hybrids and liposomes. b) UV spectra measurement of entrapped Van_DNG in the hybrids. c) TEM morphology of Van_L. d) TEM images of Van_DNL. e) Stability of the formulations at 4 °C over 4 weeks.

nanogel.

Furthermore, UV spectra analysis showed a slight red shift of 2 nm due to entrapment of vancomycin in nanogel (Fig. 4b) which disappeared following Van_DNL preparation. Subsequent disruption of the lipid bilayer with methanol resulted in the reappearance of the characteristic peak due to the release of vancomycin from Van_DNL which further supports the EE% results.

The morphology of Van_DNL was thereafter characterized by transmission electron microscopy (TEM) as a final confirmation of nanogel encapsulation. As shown in Fig. 4c, the Van_L displayed a spherical morphology with a relatively clear core containing nanocrystals (blue arrows) of low electron density potentially due to the self-aggregation of vancomycin within the lipid bilayer (red arrow). Conversely, the core-shell structure of Van_DNL (Fig. 4d) displayed a darker core (green arrow) due to negative staining of the entrapped DNA alongside a corona which can be attributable to the nanogel entrapment. Jiang and co-workers reported on the development of magnetic nucleic acid delivery system composed of a lipidoid coating [43]. TEM imaging revealed core shell nanosystem with complete and uniform coating on the nanoparticle surface as observed in our work.

To evaluate the stability of the formulation upon storage, we monitored changes in size of the formulations over 4 weeks. As shown in Fig. 4e, significant changes in the size of Van_DNG were observed over time. The significant changes in size can be attributable to the large polydispersity index of the formulations which negatively affects storage stability. Conversely, no significant difference in the hydrodynamic diameter and zeta potential was observed over 4 weeks and over 2 months (Fig. S1) for Van_DNL. Furthermore, we also observed that entrapment of vancomycin during the self-assembly of the nanogel, as reported for hybrid fabrication, further improved the stability of the formulation. This is because, the addition of vancomycin to nanogel solutions after self-assembly (post-loading) before hydrating the lipid films resulted in immediate aggregation of the liposomes upon storage at 4 °C (Fig. S2). Several examples of nanoparticulate liposomal hybrids have been developed to enhance stability and promote stimuli-responsiveness [44]. Under physiologic conditions, the encapsulation of gold nanoparticles within high density lipoproteins for instance, reduced aggregation [45]. Additionally, enhanced stability was observed when DNA was complexed with lipid coated gold nanoparticles [46,47], which is in agreement with our stability results.

3.3. *In vitro* release of vancomycin from Van_DNL hybrids

To further explore the release profile of vancomycin from the formulations under physiological conditions, *in vitro* drug release experiments were conducted. As shown in Fig. 5a, approximately 59.17 ± 13.42% of vancomycin was released within 12 h from the Van_DNG formulation. At 24 h, the total drug release was approximately 87.19 ± 8.61% for the nanogel formulation. Release of vancomycin from the Van_L formulation achieved a total drug release of 43.89 ± 4.11 by 12 h and 73.21 ± 3.0% by 24 h. This observation is attributable to the presence of vesicular structures in the liposomal formulation that reduced the release rate of vancomycin. Next, vancomycin release from Van_DNL was evaluated and shown to be significantly slower, with approximately 30.84 ± 3.86% and 52.34 ± 9.45% released by 12 h and 24 h respectively. The significant reduction in drug release from Van_DNL is attributable to the entrapment of the DNA nanogels which agrees with DLS and TEM results. Comparatively, slower release of entrapped doxorubicin from magnetic nanoparticle coated DNA nanogels was shown with approximately 25% released within 5 h which was enhanced in response to external stimuli such as pH [42]. In our hybrid, a similarly slow release of vancomycin

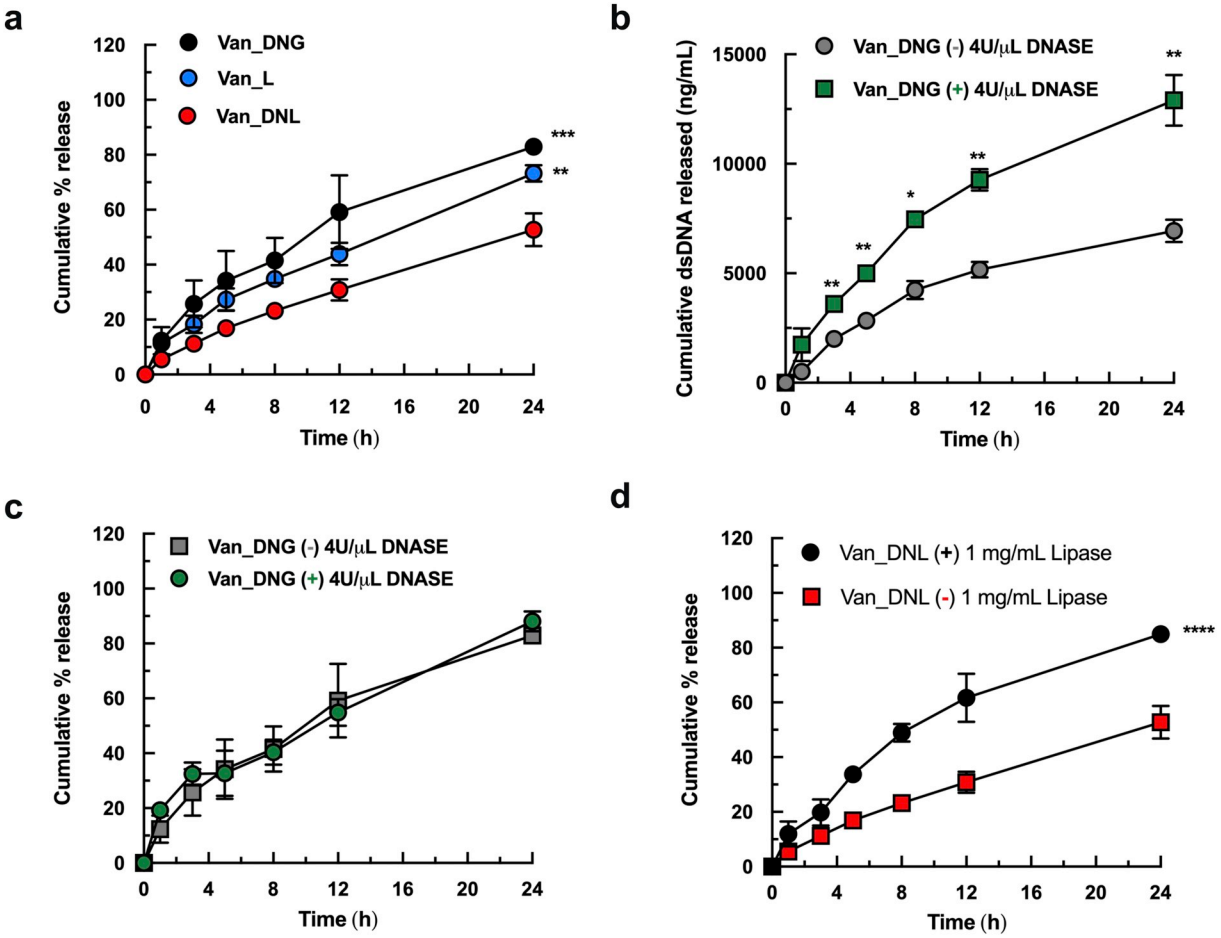

Fig. 5. *In vitro* drug release. (a) Sustained release of vancomycin from the hybrids compared to liposomal and nanogel formulations. (b) Effect of DNase on release of dsDNA from the nanogels over 24 h. (c) Effect of DNase on vancomycin release from the nanogels. (d) Controlled release of vancomycin from the hybrids in the presence and absence of lipase.

was observed which is attributable to the lipid bilayer.

Enzyme sensitive nanocarriers are attractive platforms for developing "on-demand" systems against infectious agents as they selectively induce therapeutic cargo release. Thus, to determine the enzyme responsive release profile for vancomycin from Van_DNL in comparison to Van_DNG, the accumulated release of vancomycin was evaluated in response to DNase or lipase. In Van_DNG, approximately 6933.3 ng/mL of dsDNA was released after 24 h in the absence of DNase (Fig. 5b). A significant increase in the released dsDNA to 12,900 ng/μL of dsDNA was shown in the presence of 4 U/μL of DNase. Surprisingly, despite the significant increase in dsDNA from the formulation, there was no significant difference in percentage of vancomycin released from Van_DNG was shown (Fig. 5c). On the contrary, when Van_DNL was incubated with lipase, catalytic degradation of the lipid bilayer resulted in a dramatic increase in vancomycin release. The cumulative release of vancomycin reached 33.70 ± 0.07% of the total encapsulated drug within 5 h in the presence of lipase compared to 16.91 ± 0.92 in the absence of lipase (Fig. 5d). At 24 h, drug release was further accelerated with approximately 84.97 ± 0.47% release in the presence of lipase compared to 52.34 ± 9.45% released in the absence of lipase. These findings demonstrate that release of vancomycin is better controlled from the hybrid formulation wherein active enzymes such as lipases secreted by pathogenic *S. aureus* could degrade the liposomal bilayer and trigger rapid vancomycin release. It is well-known that the hydrolysis of phospholipids can be catalysed by lipases due to the presence of ester bonds [48,49]. Our observations are in good agreement with previous studies wherein liposomal membranes were disrupted in the presence of lipases to trigger the release of entrapped cargos [50–53]. In the treatment of *Helicobacter pylori*, Thamphiwatana and coworkers exploited the abundance of secreted phospholipases within infection sites to develop a doxycycline loaded liposomal hybrid [54]. The authors demonstrated a significant increase (10× increase) in the release of rhodamine B from the hybrids in the presence of 10 μg/mL compared to 1 μg/mL of the enzyme. Additionally, six times increase in antibacterial efficacy of the hybrids was observed compared to the empty controls which was significantly reduced when a phospholipase inhibitor was added. The higher responsiveness of this hybrid (600–2400 U/mg lipase) in comparison to our system (0.1 U/mg) is attributable to the greater enzymatic activity of the lipase used by the authors. Despite the absence of control over vancomycin release in the nanogel formulation, the responsive degradation of the dsDNA is advantageous considering its therapeutic advantage in Van_DNL and highlights the dual responsiveness of the hybrid formulation to both lipase and DNase; both of which are produced by *S. aureus* [22,29].

3.4. *In vitro* antimicrobial activity

After demonstrating the lipase triggered release of vancomycin from Van_DNL, we examined the antibacterial properties of the hybrid formulation against pathogenic *S. aureus*. Vancomycin is a mainstream glycopeptide antibiotic that is reserved against resistant Gram-positive infections such as methicillin resistant *Staphylococcus aureus* (MRSA) [55,56]. We tested the antibacterial effect of the formulations against *S. aureus* by monitoring changes in bacterial viability (OD 600 nm) after

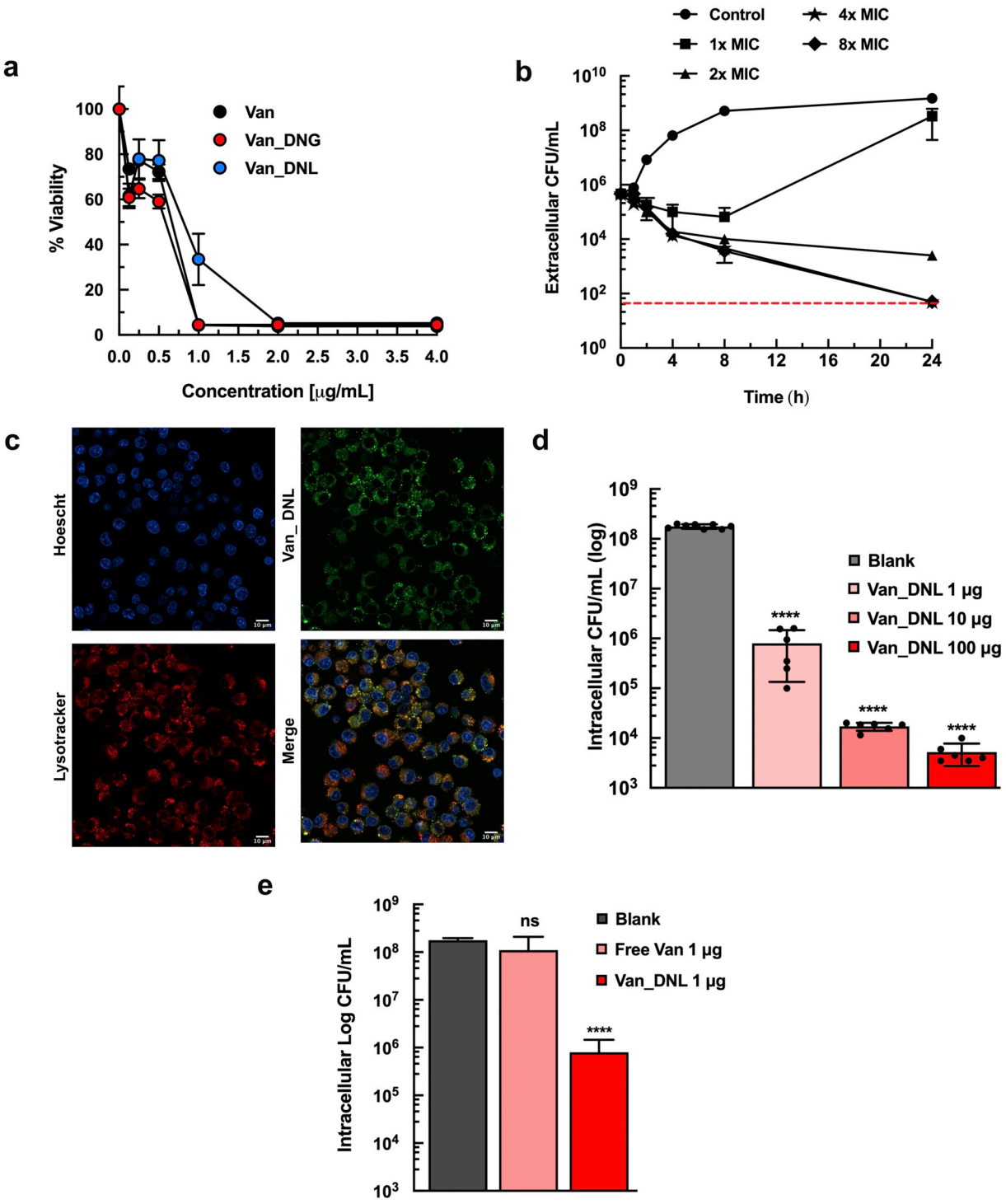

Fig. 6. *In vitro* antibacterial activity, intracellular antibacterial activity and uptake studies. (a) Effect of the free vancomycin, vancomycin loaded nanogel and vancomycin loaded hybrid formulations on bacterial cell viability measured at OD 600 nm after 18 h. (b) *In vitro* time kill kinetics of the vancomycin loaded hybrid formulations at different doses over 24 h (red dotted line refers to limit of detection). (c) Intracellular uptake of the vancomycin loaded hybrid. Nuclei stained with Hoechst, lysosomes stained with Lysotracker RED dye and hybrid stained with TopFluor dyes. (d) Intracellular antibacterial activity of the vancomycin loaded hybrid formulations at different doses in *S. aureus* infected macrophage cell model over 24 h. (e) Intracellular antibacterial activity of the vancomycin loaded hybrid formulations and free vancomycin in *S. aureus* infected macrophage cell model over 24 h. (For interpretation of the references to colour in this figure legend, the reader is referred to the web version of this article.)

treatment with different doses of free vancomycin, the nanogel formulation and the hybrid formulation. As shown in Fig. 6a, after 18 h, the free vancomycin completely inhibited the growth of *S. aureus* at a concentration of 1 μg/mL. Similar inhibitory effect was observed for the nanogel formulation due to the faster release profile and demonstrates that thermal hybridization conditions used in the fabrication of the nanogel did not degrade the drug. For the hybrid formulations, approximately 33.45 ± 19.73% viability of the bacterial cells was observed at 1 μg/mL and a higher concentration of 2 g/mL was required to completely inhibit bacterial growth. This observation could be

attributable to the sustained release of vancomycin from the hybrids and is in good agreement with the *in vitro* release data. Of the multiple enzymes produced by *S. aureus* during infections, lipases are widely recognised for their relationship with bacterial virulence [57]. In lipase-producing pathogens, growth conditions such as pH, inoculum volume/bacteria density, incubation time and carbon source have been demonstrated to influence lipase production and activity [58]. For instance, Salihu and colleagues reported that a directly proportional effect on lipase activity was observed due to the inoculum volume of the bacteria [59]. Ilesanmi and co-workers observed a similar trend with incubation time and showed maximum lipase activity after 12 h of incubation [58]. The time dependent release of virulence factors from *S. aureus* and low inoculum volume may account for the slower release of vancomycin from the hybrid as observed by the higher bacteria cell viability compared to the vancomycin loaded nanogel and free drug.

Next, we examined the time-dependent antibacterial activity of the hybrid formulation at varying doses based on the MIC (1× MIC to 8× MIC) and using a higher bacteria inoculum. As shown in Fig. 6b, a similar onset of action was observed for 2× MIC, 4× MIC and 8× MIC doses. A time dependent reduction in bacterial CFU was observed at all doses of the hybrid formulation for the first 8 h. For instance, for the 4× MIC hybrid formulation, approximately 0.6-log, 1.9-log, 3.7-log, 5.0-log and 7.5-log reduction in CFU was observed at 1 h, 2 h, 4 h, 6 h, and 8 h respectively. A concentration dependent reduction in CFU was also observed after 8 h, with approximately 3.9-log, 4.7-log, 5.0 log and 5.2-log reduction in CFU for the 1×, 2×, 4× and 8× MIC concentrations of the hybrid. After 24 h, no detectable colonies were seen for the 4× (7.5-log) and 8× (7.5-log) MIC formulations demonstrating the *in vitro* efficacy of the hybrid formulation against planktonic *S. aureus*.

3.5. Intracellular antimicrobial activity and uptake of the hybrids

Many antibiotics exhibit poor efficacy against persistent infections due to their limited intracellular penetration and poor accumulation. This restricted intracellular efficacy increases the risk of recurring infections thus, to test whether the hybrids could be used in treating intracellular infections, we tested their intracellular penetration in RAW264.7 cells. The Top-Fluor labelled Van_DNL was incubated with the cells and confocal microscopy images captured. The results revealed that Van_DNL was internalized by macrophage cells within 12 h of incubation as shown in Fig. 6c and Fig. S3. Further investigation of the uptake mechanisms revealed that following uptake, Van_DNL was associated with intracellular endosomes/lysosomes as confirmed by the colocalization with the red fluorescence of the LysoTracker Red Stain (Fig. 6c) showing that the hybrid is internalized *via* an endocytosis driven mechanism. Moreover, the confocal images also revealed that uptake of the intact Van_DNL given the presence of a Hoechst-stained core (Fig. S4) which is attributable to the presence of the DNA nanogel and is advantageous for achieving intracellular antimicrobial and anti-inflammatory activity. According to current knowledge, the ideal physicochemical properties of nanocarriers suited for efficient cellular uptake varies with cell type [60]. Of nanocarriers composed of neutral, cationic or anionic charges with sizes from 50 nm to 800 nm that have been trialed, greater uptake has been observed with smaller liposomal nanoparticles (85 nm). However, several studies have shown that the immune system generates a stronger reaction with particles less than 100 nm and that uptake into mononuclear phagocyte system (MPS) cells can be improved by increasing nanocarrier size with optimal sizes of 200 nm reported [61]. While, carriers with cationic and anionic surface charges have been shown to be associated with efficient cellular uptake, the cytotoxicity of cationic nanocarriers limits their clinical use [62]. On the other hand, repulsive forces are imminent between the anionic liposomes and the DNA nanogels. In comparison to recent reports, Yao and colleagues investigated the intracellular delivery of magnetic DNA nanogels with similar size distribution (216 ± 25 nm) [42]. Greater uptake efficiency was observed after 12 h and 24 h which was comparable to the hybrids.

The intracellular antimicrobial activity of Van_DNL was evaluated by examining the survival of intracellular *S. aureus* after treatment with different doses of the formulation and to further reveal that the hybrid could release its drug content in infected cells. We used *S. aureus* infected Raw264.7 cells, a murine macrophage cell line, and evaluated the intracellular survival of *S. aureus*. Treatment with Van_DNL achieved a concentration dependent reduction in the intracellular bacteria growth after 24 h of incubation as shown in Fig. 6d. The blank hybrid formulation, DNL had no inhibitory effect on the bacteria growth and was comparable to the placebo control (Fig. S5). Intracellular bacterial infection within the cells after eliminating extracellular bacteria for DNL after 24 h was shown to be approximately $10^{8.11}$ (n = 8). All concentration of Van_DNL resulted in significant reduction in bacteria CFU. At 1 μg/mL absolute concentration of Van_DNL, a 2.35-log significant reduction in bacteria CFU was observed. It is worth noting that, treatment with the free drug resulted in only 0.21-log reduction in CFU at this concentration of vancomycin (Fig. 6e) demonstrating the superior antimicrobial activity of Van_DNL. At higher concentrations of 10 μg/mL and 100 μg/mL Van_DNL, a 4-log and 4.5-log reduction in bacterial CFU respectively, was observed which corresponds to 99.99% inhibition in bacteria growth intracellularly. Evaluation of the extracellular bacteria revealed a significant reduction in extracellular bacteria with no viable bacteria colonies in comparison to the controls at 100 μg/mL dose of the hybrid (Fig. S6). The dose dependent reduction in intracellular bacteria observed is attributable to the intracellular release of entrapped vancomycin which agrees with the results from the *in vitro* release and time kill kinetics. Moreover, the results clearly demonstrate that Van_DNL could be delivered intact into macrophage cells, release encapsulated vancomycin to efficiently kill intracellular *S. aureus*. We observed no significant difference between the potency of Van_L and the Van_DNL (Fig. S7).

3.6. Biocompatibility, anti-inflammatory and anti-oxidant effect of the hybrid

We then evaluated the biocompatibility of the blank and vancomycin loaded hybrid formulations in RAW264.7 cells. As shown in Fig. 7a, treatment with Van_DNL resulted in more than 70% cellular viability demonstrating the non-toxicity of the formulations according to ISO criteria [63]. After 48 h the observed cellular viability was 80.16 ± 6.2% (12.5 μg/mL), 83.0 ± 11.77% (25 μg/mL), 95.25 ± 14.02% (50 μg/mL) and 89.79 ± 7.90% (100 μg/mL) for the various concentrations tested. Treatments with equal volumes of DNL resulted in cell viabilities between 99.99 ± 23.40% and 118.17 ± 19.75% demonstrating that the hybrid formulations did not cause significant toxicity to the cells which is attributable to the biocompatibility of the DNA nanostructures/ natural phospholipids and their degradation products [64,65]. The observed high cytocompatibility of the hybrids is in good agreement with similar nano-constructs. For instance, Ternullo and colleagues studied the effect of Lipoid S based liposomes on human foreskin fibroblasts and human immortalised keratinocytes [34]. The authors reported increased viability in these cell lines after 24 h of treatment. Recently, Thelu and co-workers also showed negligible toxicity of DNA hybrid nanogels against Ramos, HeLa and CCRF-CEM cells [66]. Using the CCK8 assay, Mao and colleagues treated human dermal fibroblasts with DNA tetrahedral nanostructures for 24 h [67]. The authors revealed that the cell viability significantly increased and peaked at 250 nM (>100%). These high cell viabilities have been reported by several other authors [22] which agrees with our results.

Several lines of evidence suggest that inflammatory response to bacterial infection can be due to bacterial cell components such as lipopolysaccharides (LPS), lipoteichoic acid (LTA) and peptidoglycan

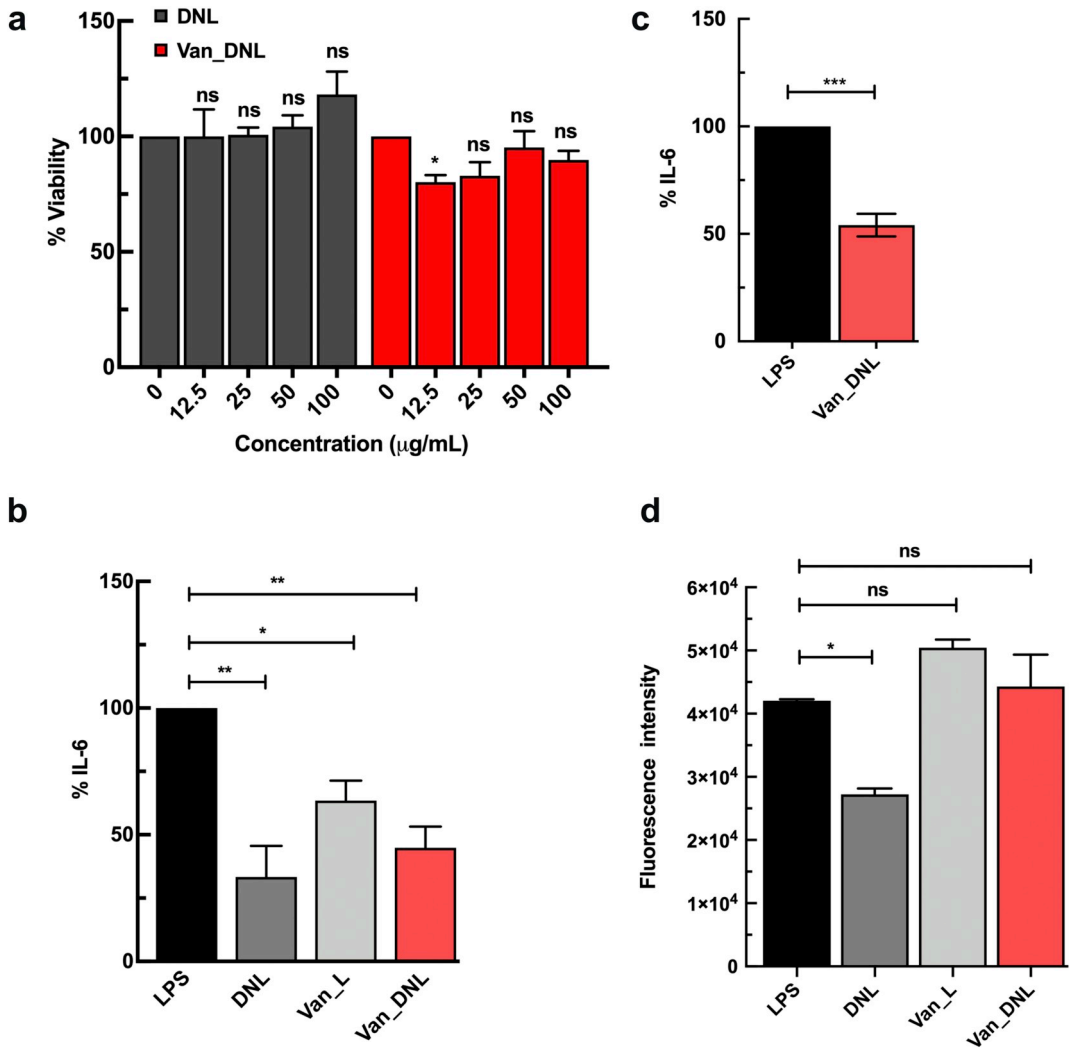

Fig. 7. *In vitro* biocompatibility, anti-inflammatory and anti-oxidant activity of the hybrid. (a) Cytocompatibility of the blank and vancomycin loaded hybrid formulation against RAW264.7 macrophages over 48 h. (b) *In vitro* anti-inflammatory activity of the blank hybrid formulation, vancomycin loaded liposomal and vancomycin loaded hybrid formulations after pre-treatment in LPS stimulated macrophages. (c) *In vitro* anti-inflammatory activity of the vancomycin loaded hybrid formulations after co-treatment in LPS stimulated macrophages. (d) *In vitro* effect on ROS production of the blank hybrid formulation, vancomycin loaded liposomal and vancomycin loaded hybrid formulations after pre-treatment in LPS stimulated macrophages.

(PepG) which induce inflammation [68]. Thus, to better understand the effect of the hybrid on inflammatory response, we established an LPS activated macrophage cell models using RAW264.7 cells. The cells were either pre-treated with the formulations prior to LPS stimulation (pre-treatment) to determine if they could function as a preventive strategy or treated together with LPS (co-treatment) to determine if they could be used minimize inflammation. We compared the inflammatory response of the blank nanogel, vancomycin loaded liposomal and vancomycin loaded hybrid formulations by measuring changes in IL-6 production. As shown in Fig. 7b, LPS stimulation caused a significant increase in IL-6 production. Pre-treatment of the macrophage cells with the DNL prevented this inflammatory response, resulting in approximately 66.67 ± 21.19% reduction in IL-6 release ($p < .01$).

This observation is attributable to the potent anti-inflammatory activity of the DNA nanostructures and is in good agreement with previous studies [16,22]. Treatment with the Van_L resulted in only 36.51 ± 13.59% reduction in IL-6 release which was significantly lesser than DNL. This observed is attributable to the reported anti-inflammatory activity of vancomycin [69].Van_DNL treatment resulted in 55.14 ± 14.45% reduction in IL-6 release ($p < .01$), which was significantly greater than the observed reduction for Van_L ($p < .05$). These results further indicate that Van_DNL nanocarriers potentiated the anti-inflammatory activity of the cargo and highlight its synergistic anti-inflammatory efficacy. Co-treatment of the cells with Van_DNL during endotoxin stimulation, similarly exerted a potent anti-inflammatory effect with 45.94 ± 5.29% (Fig. 7c) reduction in IL-6 production which notably demonstrates that the hybrid formulation can be used as an immune modulatory agent. *S. aureus* infections are commonly associated with bacterial skin infections, bacteraemia, peritonitis and septic shock [70]. The release of potent pro-inflammatory cytokines such as tumour necrosis factor alpha and interleukin-6 causes severe inflammatory responses during *S. aureus* infection. This overwhelming uncontrolled inflammation (cytokine storm) causes multi-organ failure which is the hallmark of *Staphylococcal* toxic shock syndrome [70]. Antibiotics such as vancomycin are considered as one of the main measures in eradicating the pathogen. In addition to reducing bacteria growth, vancomycin has been shown to substantially decrease inflammatory markers such as TNF-a and IL-6 [69]. In this study, we demonstrated that while the use of liposomal vancomycin alone led to a significant reduction in IL-6 production, this was to a lesser extent that the anti-inflammatory activity achieved with the DNA nanogel. In line with growing interest in crosslinked DNA nanostructures as anti-inflammatory agents, a recent study by Zhang and co-workers showed that pre-treatment with tetrahedral DNA

nanostructures in macrophages resulted in a significant reduction in IL-6 production ($p < .01$) after 24 h [16]. Similarly, our previous work demonstrated reduced LPS induced inflammation (22.8 ± 9.15%) in macrophages with crosslinked DNA nanostructures [22]. This observation was clinically significant as it translated into rapid enhancement of wound closure in murine mouse models. Thus, we hypothesized that the best therapeutic can be offered by the combination of the nanocarriers with antibiotics. Gao et al. recently developed a peptide-gold nanoparticulate hybrid and examined their anti-inflammatory activity [71]. *In vitro*, the authors demonstrated a potent inhibitory activity ($p < .01$) of the hybrids on downstream cytokine production in THP-1 cell derived macrophages. The most potent hybrid prolonged the survival of mice experiencing lethal LPS challenge *via* reduced lung inflammation and by alleviating diffuse alveolar damage. The observed comparable potent synergism ($p < .01$) of the hybrid thus paves way to address the clinical manifestation of inflammation.

Next, the antioxidant effect of Van_DNL was evaluated by monitoring oxidative stress as a function of reactive oxygen species (ROS) and the changes in the DCFH-DA fluorescent probes. As previously reported, the production of ROS oxidizes the nonfluorescent DCFH-DA probe to emit a green fluorescence [72]. As shown in Fig. 7d, LPS stimulation resulted in a significant increase in ROS production with a quantified fluorescence intensity of 42,046 ± 243.24. Pre-treatment with DNL led to a significant reduction in ROS production and corresponding fluorescence intensity of 27,241.5 ± 912.87. Conversely, we recorded a fluorescence intensity of 50,429 ± 1288.35 for Van_L attributable to the release of vancomycin, which is known to increase intracellular ROS production as a part of its mechanism of action against pathogenic bacteria [73]. Similarly, treatment with Van_DNL resulted in approximately 44,316 ± 5027.5 release of ROS which was not significantly different from the liposomal formulation. These results clearly confirm the intracellular release of vancomycin from Van_DNL and also demonstrate that, the potent antioxidant effect of the DNL does not diminish the ROS mediated antibacterial activity of vancomycin *in vitro*.

4. Conclusion

An innovative hybrid formulation, Van_DNL, composed of DNA nanogels encapsulated in liposomal vesicles was fabricated as a universal loading platform for the intracellular delivery of antibiotics. The self-assembly of the DNA nanostructures, loading of vancomycin *via* non-covalent electrostatic interactions and subsequent hydration of a lipid film endowed the hybrid formulation with an anti-inflammatory DNA nanogel core and “on-demand” release feature imparted by the lipid bilayer. The binding affinity between the DNA nanostructures and vancomycin was shown to significantly increase the antibiotic loading and resulted in a relatively slower release profile than the liposomal or nanogel formulations alone. We demonstrated enzyme potentiated release of vancomycin from Van_DNL in response to lipase enzymes whilst DNase treatment resulted in a faster degradation of the nanostructures but not vancomycin. *In vitro* antibacterial activity of Van_DNL demonstrated a dose dependent and time-dependent reduction in CFU of planktonic bacteria. The intracellular uptake of Van_DNL was shown to be *via* an endocytosis mediated mechanism which translated into a significant reduction in intracellular and extracellular bacterial CFU in a dose dependent manner. Furthermore, the intracellular transport of Van_DNL resulted in a significant anti-inflammatory activity in LPS treated raw macrophages which was synergistic with the anti-inflammatory activity of vancomycin. Finally, we demonstrated that the potent anti-oxidant effect of the blank hybrid, DNL, did not disrupt the ROS induced mechanism of the antimicrobial cargo. Our results clearly highlight the tremendous potential of the hybrid as an innovative antibacterial nanocarrier and a powerful multifunctional co-delivery platform which can be broadly applied against persistent infections. For future directions implementing pathogen and cell targeting in clinical models of infection/inflammation and demonstrating potency against more virulent strains using functionalized hybrids will be explored.

Acknowledgment

This project has received funding from the European Union’s Horizon 2020 research and innovation programme under the Marie Skłodowska-Curie grant agreement No 834811. The authors acknowledge research facilities at UIT The Arctic University of Norway (Department of Pharmacy, Advanced Microscopy Core Facility and Department of Medical Biology) and would like to thank Prof. Pål J. Johnsen for support with research equipment for the preparation of the hybrids. We thank Lipoid GmbH (Germany) for providing Lipoid S100 for the project. Schematic diagram acknowledgement to Vanitha Selvarajan (Department of Pharmacy, National University of Singapore, Singapore) and S. Obuobi.

Appendix A. Supplementary data

Supplementary data to this article can be found online at https://doi.org/10.1016/j.jconrel.2020.06.002.

References

[1] WHO, Antimicrobial Resistance, Global Report on Surveillance 2014, (2014), p. 257.
[2] J. Kluytmans, A. van Belkum, H. Verbrugh, Nasal carriage of Staphylococcus aureus: epidemiology, underlying mechanisms, and associated risks, Clin. Microbiol. Rev. 10 (1997) 505–520.
[3] C. Garzoni, W.L. Kelley, Staphylococcus aureus: new evidence for intracellular persistence, Trends Microbiol. 17 (2009) 59–65.
[4] X. Wang, X. Wang, D. Teng, R. Mao, Y. Hao, N. Yang, Z. Li, J. Wang, Increased intracellular activity of MP1102 and NZ2114 against Staphylococcus aureus in vitro and in vivo, Sci. Rep. 8 (2018) 4204.
[5] N. Abed, P. Couvreur, Nanocarriers for antibiotics: a promising solution to treat intracellular bacterial infections, Int. J. Antimicrob. Agents 43 (2014) 485–496.
[6] J.K. Patra, G. Das, L.F. Fraceto, E.V.R. Campos, M.D.P. Rodriguez-Torres, L.S. Acosta-Torres, L.A. Diaz-Torres, R. Grillo, M.K. Swamy, S. Sharma, S. Habtemariam, H.S. Shin, Nano based drug delivery systems: recent developments and future prospects, J. Nanobiotechnol. 16 (2018) 71.
[7] S. Hallaj-Nezhadi, M. Hassan, Nanoliposome-based antibacterial drug delivery, Drug Deliv. 22 (2015) 581–589.
[8] F.Y. Su, J. Chen, H.N. Son, A.M. Kelly, A.J. Convertine, T.E. West, S.J. Skerrett, D.M. Ratner, P.S. Stayton, Polymer-augmented liposomes enhancing antibiotic delivery against intracellular infections, Biomater. Sci. 6 (2018) 1976–1985.
[9] I.V. Zhigaltsev, N. Maurer, Q.F. Akhong, R. Leone, E. Leng, J. Wang, S.C. Semple, P.R. Cullis, Liposome-encapsulated vincristine, vinblastine and vinorelbine: a comparative study of drug loading and retention, J. Control. Release 104 (2005) 103–111.
[10] S. Sur, A.C. Fries, K.W. Kinzler, S. Zhou, B. Vogelstein, Remote loading of preencapsulated drugs into stealth liposomes, Proc. Natl. Acad. Sci. U. S. A. 111 (2014) 2283–2288.
[11] P.A. Burnouf, Y.L. Leu, Y.C. Su, K. Wu, W.C. Lin, S.R. Roffler, Reversible glycosidic switch for secure delivery of molecular nanocargos, Nat. Commun. 9 (2018) 1843.
[12] I. Eroglu, M. Ibrahim, Liposome-ligand conjugates: a review on the current state of art, J. Drug Target. 28 (2020) 225–244.
[13] M.I. Setyawati, R.V. Kutty, C.Y. Tay, X. Yuan, J. Xie, D.T. Leong, Novel theranostic DNA nanoscaffolds for the simultaneous detection and killing of Escherichia coli and Staphylococcus aureus, ACS Appl. Mater. Interfaces 6 (2014) 21822–21831.
[14] Q. Hu, H. Li, L. Wang, H. Gu, C. Fan, DNA nanotechnology-enabled drug delivery systems, Chem. Rev. 119 (2019) 6459–6506.
[15] J. Li, C. Zheng, S. Cansiz, C. Wu, J. Xu, C. Cui, Y. Liu, W. Hou, Y. Wang, L. Zhang, I.T. Teng, H.H. Yang, W. Tan, Self-assembly of DNA nanohydrogels with controllable size and stimuli-responsive property for targeted gene regulation therapy, J. Am. Chem. Soc. 137 (2015) 1412–1415.
[16] Q. Zhang, S. Lin, S. Shi, T. Zhang, Q. Ma, T. Tian, T. Zhou, X. Cai, Y. Lin, Anti-inflammatory and antioxidative effects of tetrahedral DNA nanostructures via the modulation of macrophage responses, ACS Appl. Mater. Interfaces 10 (2018) 3421–3430.
[17] Y. Hu, Z. Chen, H. Zhang, M. Li, Z. Hou, X. Luo, X. Xue, Development of DNA tetrahedron-based drug delivery system, Drug Deliv. 24 (2017) 1295–1301.
[18] L. Zhang, S.R. Jean, S. Ahmed, P.M. Aldridge, X. Li, F. Fan, E.H. Sargent, S.O. Kelley, Multifunctional quantum dot DNA hydrogels, Nat. Commun. 8 (2017) 381.
[19] Y.X. Zhao, A. Shaw, X. Zeng, E. Benson, A.M. Nystrom, B. Hogberg, DNA origami delivery system for cancer therapy with tunable release properties, ACS Nano 6 (2012) 8684–8691.
[20] Q. Jiang, C. Song, J. Nangreave, X.W. Liu, L. Lin, D.L. Qiu, Z.G. Wang, G.Z. Zou,

X.J. Liang, H. Yan, B.Q. Ding, DNA origami as a carrier for circumvention of drug resistance, J. Am. Chem. Soc. 134 (2012) 13396–13403.
[21] X. Xu, S. Fang, Y. Zhuang, S. Wu, Q. Pan, L. Li, X. Wang, X. Sun, B. Liu, Y. Wu, Cationic albumin encapsulated DNA origami for enhanced cellular transfection and stability, Materials (Basel) 12 (2019).
[22] S. Obuobi, H.K. Tay, N.D.T. Tram, V. Selvarajan, J.S. Khara, Y. Wang, P.L.R. Ee, Facile and efficient encapsulation of antimicrobial peptides via crosslinked DNA nanostructures and their application in wound therapy, J. Control. Release 313 (2019) 120–130.
[23] Y. Li, Z. Wang, Q. Wei, M. Luo, G. Huang, B.D. Sumer, J. Gao, Non-covalent interactions in controlling pH-responsive behaviors of self-assembled nanosystems, Polym. Chem. 7 (2016) 5949–5956.
[24] C.R. Thorn, A.J. Clulow, B.J. Boyd, C.A. Prestidge, N. Thomas, Bacterial lipase triggers the release of antibiotics from digestible liquid crystal nanoparticles, J. Control. Release 319 (2020) 168–182.
[25] K.E. Jaeger, S. Ransac, B.W. Dijkstra, C. Colson, M. van Heuvel, O. Misset, Bacterial lipases, FEMS Microbiol. Rev. 15 (1994) 29–63.
[26] S. Yang, X. Han, Y. Yang, H. Qiao, Z. Yu, Y. Liu, J. Wang, T. Tang, Bacteria-targeting nanoparticles with microenvironment-responsive antibiotic release to eliminate intracellular Staphylococcus aureus and associated infection, ACS Appl. Mater. Interfaces 10 (2018) 14299–14311.
[27] W. Sun, T. Jiang, Y. Lu, M. Reiff, R. Mo, Z. Gu, Cocoon-like self-degradable DNA nanoclew for anticancer drug delivery, J. Am. Chem. Soc. 136 (2014) 14722–14725.
[28] M. Chen, S. Xie, J. Wei, X. Song, Z. Ding, X. Li, Antibacterial micelles with Vancomycin-mediated targeting and pH/lipase-triggered release of antibiotics, ACS Appl. Mater. Interfaces 10 (2018) 36814–36823.
[29] M.H. Xiong, Y. Bao, X.Z. Yang, Y.C. Wang, B. Sun, J. Wang, Lipase-sensitive polymeric triple-layered nanogel for "on-demand" drug delivery, J. Am. Chem. Soc. 134 (2012) 4355–4362.
[30] G. Pan, Q. Mou, Y. Ma, F. Ding, J. Zhang, Y. Guo, X. Huang, Q. Li, X. Zhu, C. Zhang, pH-responsive and gemcitabine-containing DNA nanogel to facilitate the chemodrug delivery, ACS Appl. Mater. Interfaces 11 (2019) 41082–41090.
[31] Z. Chen, F. Liu, Y. Chen, J. Liu, X. Wang, A.T. Chen, G. Deng, H. Zhang, J. Liu, Z. Hong, J. Zhou, Targeted delivery of CRISPR/Cas9-mediated cancer gene therapy via liposome-templated hydrogel nanoparticles, Adv. Funct. Mater. 27 (2017).
[32] S.D. Perrault, W.M. Shih, Virus-inspired membrane encapsulation of DNA nanostructures to achieve in vivo stability, ACS Nano 8 (2014) 5132–5140.
[33] S. Ternullo, E. Gagnat, K. Julin, M. Johannessen, P. Basnet, Z. Vanic, N. Skalko-Basnet, Liposomes augment biological benefits of curcumin for multitargeted skin therapy, Eur. J. Pharm. Biopharm. 144 (2019) 154–164.
[34] S. Ternullo, P. Basnet, A.M. Holsaeter, G.E. Flaten, L. de Weerd, N. Skalko-Basnet, Deformable liposomes for skin therapy with human epidermal growth factor: the effect of liposomal surface charge, Eur. J. Pharm. Sci. 125 (2018) 163–171.
[35] S. Obuobi, Y. Wang, J.S. Khara, A. Riegger, S.L. Kuan, P.L.R. Ee, Antimicrobial and anti-biofilm activities of surface engineered polycationic albumin nanoparticles with reduced hemolytic activity, Macromol. Biosci. 18 (2018) e1800196.
[36] H. Xue, F. Ding, J. Zhang, Y. Guo, X. Gao, J. Feng, X. Zhu, C. Zhang, DNA tetrahedron-based nanogels for siRNA delivery and gene silencing, Chem. Commun. (Camb.) 55 (2019) 4222–4225.
[37] S.K.A. Hari Veera Prasad Thelu, Murali Golla, Nithiyanandan Krishnan, Divya Ram, S. Murty Srinivasula, Reji Varghese, Size controllable DNA nanogels from the self-assembly of DNA nanostructures through multivalent host–guest interactions, Nanoscale 10 (2018) 222–230.
[38] H. Tun, Sequence-independent DNA nanogel as a potential drug carrier, Macromol. Rapid Commun. 38 (2017) 1–10.
[39] M.H. Xiong, Y.J. Li, Y. Bao, X.Z. Yang, B. Hu, J. Wang, Bacteria-responsive multifunctional nanogel for targeted antibiotic delivery, Adv. Mater. 24 (2012) 6175–6180.
[40] L. Kong, Z.F. Liu, S.P. Liu, D.F. Wang, Interaction of vancomycin with DNA, and determination of DNA via resonance Rayleigh scattering and resonance nonlinear scattering, Anal. Methods UK 4 (2012) 4346–4352.
[41] N. Doroshenko, B.S. Tseng, R.P. Howlin, J. Deacon, J.A. Wharton, P.J. Thurner, B.F. Gilmore, M.R. Parsek, P. Stoodley, Extracellular DNA impedes the transport of vancomycin in Staphylococcus epidermidis biofilms preexposed to subinhibitory concentrations of vancomycin, Antimicrob. Agents Chemother. 58 (2014) 7273–7282.
[42] Y.Y. Chi Yao, Dayong Yang, Magnetic DNA nanogels for targeting delivery and multi-stimuli triggered release of anticancer drugs, ACS Appl. Bio Mater. 1 (2018) 2012–2020.
[43] S. Jiang, A.A. Eltoukhy, K.T. Love, R. Langer, D.G. Anderson, Lipidoid-coated iron oxide nanoparticles for efficient DNA and siRNA delivery, Nano Lett. 13 (2013) 1059–1064.
[44] Z. Al-Ahmady, N. Lozano, K.C. Mei, W.T. Al-Jamal, K. Kostarelos, Engineering thermosensitive liposome-nanoparticle hybrids loaded with doxorubicin for heat-triggered drug release, Int. J. Pharm. 514 (2016) 133–141.
[45] S.T. Chuang, Y.S. Shon, V. Narayanaswami, Apolipoprotein E3-mediated cellular uptake of reconstituted high-density lipoprotein bearing core 3, 10, or 17 nm hydrophobic gold nanoparticles, Int. J. Nanomedicine 12 (2017) 8495–8510.
[46] G. Han, N.S. Chari, A. Verma, R. Hong, C.T. Martin, V.M. Rotello, Controlled recovery of the transcription of nanoparticle-bound DNA by intracellular concentrations of glutathione, Bioconjug. Chem. 16 (2005) 1356–1359.
[47] L. Zhang, X. Sun, Y. Song, X. Jiang, S. Dong, E. Wang, Didodecyldimethylammonium bromide lipid bilayer-protected gold nanoparticles: synthesis, characterization, and self-assembly, Langmuir 22 (2006) 2838–2843.
[48] P. Adlercreutz, Immobilisation and application of lipases in organic media, Chem. Soc. Rev. 42 (2013) 6406–6436.
[49] T. Mnasri, J. Herault, L. Gauvry, C. Loiseau, L. Poisson, F. Ergan, G. Pencreac'h, Lipase-Catalyzed Production of Lysophospholipids, Ocl Oils Fat Crop Li, 24 (2017).
[50] H. He, Y. Lu, J. Qi, Q. Zhu, Z. Chen, W. Wu, Adapting liposomes for oral drug delivery, Acta Pharm. Sin. B 9 (2019) 36–48.
[51] C.J.D.G.D. Sprott, L.P. Fleming, G.B. Patel, Stability of liposomes prepared from archaeobacterical lipids and phosphatidylcholine mixtures, Cell Mater. 6 (1996) 143–155.
[52] V.F.-V. Heather Ewing, Timothy P. Spicer, Peter Chase, Steven Brown, Louis Scampavia, William R. Roush, Sean Riley, Hugh Rosen, Peter Hodder, Gerard Lambeau, Michael H. Gelb, Fluorometric high-throughput screening assay for secreted phospholipases A2 using phospholipid vesicles, J. Biomol. Screen. 21 (2016) 713–721.
[53] A.H.H. Ahmad Arouri, Thomas Elmelund Rasmussen, Ole G. Mouritsen, Lipases, liposomes and lipid-prodrugs, Curr. Opin. Colloid Interface Sci. 18 (2013) 419–431.
[54] S. Thamphiwatana, W. Gao, D. Pornpattananangkul, Q. Zhang, V. Fu, J. Li, J. Li, M. Obonyo, L. Zhang, Phospholipase A2-responsive antibiotic delivery via nanoparticle-stabilized liposomes for the treatment of bacterial infection, J. Mater. Chem. B 2 (2014) 8201–8207.
[55] M.A.T. Blaskovich, K.A. Hansford, M.S. Butler, Z. Jia, A.E. Mark, M.A. Cooper, Developments in glycopeptide antibiotics, ACS Infect. Dis. 4 (2018) 715–735.
[56] M.A.T. Blaskovich, K.A. Hansford, Y. Gong, M.S. Butler, C. Muldoon, J.X. Huang, S. Ramu, A.B. Silva, M. Cheng, A.M. Kavanagh, Z. Ziora, R. Premraj, F. Lindahl, T.A. Bradford, J.C. Lee, T. Karoli, R. Pelingon, D.J. Edwards, M. Amado, A.G. Elliott, W. Phetsang, N.H. Daud, J.E. Deecke, H.E. Sidjabat, S. Ramaologa, J. Zuegg, J.R. Betley, A.P.G. Beevers, R.A.G. Smith, J.A. Roberts, D.L. Paterson, M.A. Cooper, Protein-inspired antibiotics active against vancomycin- and daptomycin-resistant bacteria, Nat. Commun. 9 (2018) 22.
[57] N.X. Chunyan Hu, Yong Zhang, Simon Rayner, Shiyun Chen, Functional characterization of lipase in the pathogenesis of Staphylococcus aureus, Biochem. Biophys. Res. Commun. 419 (2012) 617–620.
[58] A.E.A. Oluwaseye I Ilesanmi, Japhel A. Omolaiye, Efemena M. Olorode, Adebayo L. Ogunkanmi, Isolation, optimization and molecular characterization of lipase producing bacteria from contaminated soil, Scientific Afr. 8 (2020) e00279.
[59] A. Salihu, M.Z. Alam, M.I. AbdulKarim, H.M. Salleh, Lipase production: an insight in the utilization of renewable agricultural residues, Resour. Conserv. Recycl. 58 (2012) 36–44.
[60] H. Epstein-Barash, D. Gutman, E. Markovsky, G. Mishan-Eisenberg, N. Koroukhov, J. Szebeni, G. Golomb, Physicochemical parameters affecting liposomal bisphosphonates bioactivity for restenosis therapy: internalization, cell inhibition, activation of cytokines and complement, and mechanism of cell death, J. Control. Release 146 (2010) 182–195.
[61] C. Kelly, C. Jefferies, S.A. Cryan, Targeted liposomal drug delivery to monocytes and macrophages, J. Drug Deliv. 2011 (2011) 727241.
[62] H. Lv, S. Zhang, B. Wang, S. Cui, J. Yan, Toxicity of cationic lipids and cationic polymers in gene delivery, J. Control. Release 114 (2006) 100–109.
[63] G.K. Srivastava, M.L. Alonso-Alonso, I. Fernandez-Bueno, M.T. Garcia-Gutierrez, F. Rull, J. Medina, R.M. Coco, J.C. Pastor, Comparison between direct contact and extract exposure methods for PFO cytotoxicity evaluation, Sci. Rep. UK 8 (2018).
[64] K.E. Bujold, A. Lacroix, H.F. Sleiman, DNA nanostructures at the interface with biology, Chem-US 4 (2018) 495–521.
[65] J. Li, X.L. Wang, T. Zhang, C.L. Wang, Z.J. Huang, X. Luo, Y.H. Deng, A review on phospholipids and their main applications in drug delivery systems, Asian J. Pharm. Sci. 10 (2015) 81–98.
[66] S.A. Hari Veera Prasad Thelu, Devanathan Perumal, Kaloor S. Harikrishnan, Shajesh Vijayan, Reji Varghese, Self-assembly of an aptamer-decorated, DNA–protein hybrid nanogel: a biocompatible nanocarrier for targeted cancer therapy, ACS Appl. Biomater. 2 (2019) 5227–5234.
[67] C. Mao, W. Pan, X. Shao, W. Ma, Y. Zhang, Y. Zhan, Y. Gao, Y. Lin, The clearance effect of tetrahedral DNA nanostructures on senescent human dermal fibroblasts, ACS Appl. Mater. Interfaces 11 (2019) 1942–1950.
[68] K. Dickson, C. Lehmann, Inflammatory response to different toxins in experimental sepsis models, Int. J. Mol. Sci. 20 (2019).
[69] P. Zhou, D. Xia, Y. Xia, H. Zhang, Y. Wang, T. Tang, S. Xu, Synergistic effect of vancomycin and l-homocarnosine alleviates Staphylococcus aureus-induced osteomyelitis in rats, Biomed. Pharmacother. 111 (2019) 31–35.
[70] Z. Li, A.G. Peres, A.C. Damian, J. Madrenas, Immunomodulation and disease tolerance to Staphylococcus aureus, Pathogens 4 (2015) 793–815.
[71] W. Gao, Y. Wang, Y. Xiong, L. Sun, L. Wang, K. Wang, H.Y. Lu, A. Bao, S.E. Turvey, Q. Li, H. Yang, Size-dependent anti-inflammatory activity of a peptide-gold nanoparticle hybrid in vitro and in a mouse model of acute lung injury, Acta Biomater. 85 (2019) 203–217.
[72] M.D. Yinfeng Zhang, Zonghui Yuan, Methods for the detection of reactive oxygen species, Anal. Methods 10 (2018) 4625–4638.
[73] Y. Sakamoto, T. Yano, Y. Hanada, A. Takeshita, F. Inagaki, S. Masuda, N. Matsunaga, S. Koyanagi, S. Ohdo, Vancomycin induces reactive oxygen species-dependent apoptosis via mitochondrial cardiolipin peroxidation in renal tubular epithelial cells, Eur. J. Pharmacol. 800 (2017) 48–56.